

Electronic Supplementary Information

Cation exchange based electrochemical sensor for
cetyltrimethylammonium bromide detection using acridine
orange/polystyrene sulfonate system

Xia Hao, Zhen Xu, Na Li, Nian Bing Li* and Hong Qun Luo*

*Key Laboratory of Eco-environments in Three Gorges Reservoir Region (Ministry of Education),
School of Chemistry and Chemical Engineering, Southwest University, Chongqing 400715,
China*

*Corresponding author: Fax: (+86)23-6825-3237; Tel: (+86)23-6825-3237

E-mail address: linb@swu.edu.cn, luohq@swu.edu.cn

Contents

1. Characteristics of IR spectra of the system.....	3
2. Optimization of experimental parameters.....	5
2.1. Optimization of the PSS concentration	5
2.2. Optimization of the pH of AO solution	5
2.3. Optimization of the reaction time of CTAB	6
2.4. Optimization of the pH of buffer solution.....	6
3. Stability of the sensor.....	8
4. Comparison to other detection methods (Table S1).....	9
References.....	10

1. Characteristics of IR spectra of the system

To further confirm these different affinities of the PSS toward CTAB and AO, FT-IR spectroscopy was conducted. Fig.S1A displays the FT-IR spectra of PSS (black curve), AO (red curve), and AO/PSS (blue curve). As shown in Fig. S1A, AO exhibits strong absorption at 1645 cm^{-1} , which was assigned to the C=N stretching vibration, while for the AO/PSS complex, this peak was redshifted to 1639 cm^{-1} . Meanwhile, the characteristic peaks of PSS at 1185 , 1128 , and 835 cm^{-1} (black curve), which were assigned to the S=O stretching vibration, were also shifted to 1178 , 1127 , and 836 cm^{-1} (blue curve), after forming the complex with AO. These results indicated that there was an interaction between the AO and PSS, such as the electrostatic interaction. CTAB could also form a stable complex with PSS, possibly through a strong surface interaction and electrostatic interactions. This strong interaction could also induce the shift of the characteristic peak of PSS and CTAB. It can be seen from Fig.S1B that the characteristic peaks for CTAB at 1013 and 1042 cm^{-1} (black curve), which were attributed to the stretching vibration of the C-N bonds, shifted to 1010 and 1040 cm^{-1} , respectively, for the PSS/CTAB complex (red curve). To verify the different affinities of CTAB and AO with PSS, the cation exchange experiments were conducted by adding the CTAB to the AO/PSS system. Blue curve in Fig.S1B shows the FT-IR spectra of the composite of AO/PSS after exchanging with CTAB, in which the typical peaks for the PSS/CTAB complex at 1040 and 1010 cm^{-1} were observed, but the characteristic peak of the AO/PSS complex at 1639 cm^{-1} was not observed. This could elucidate that the combination of AO and PSS was weak and the strong

interaction between CTAB and PSS resulted in the dissociation of the AO/PSS complex. All these results strongly suggest that, although both AO and CTAB could interact with the PSS to form the complex, respectively, the strong electrostatic interaction between CTAB and PSS, and the hydrophobicity of CTAB might endow a stronger affinity of CTAB for PSS than that of AO.

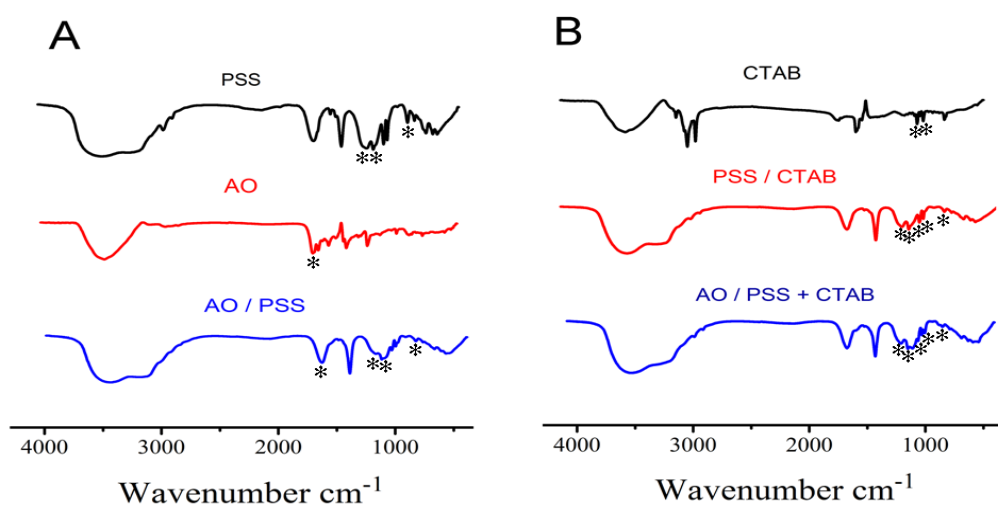


Fig. S1. (A) FT-IR spectra of pure PSS (black curve), pure AO (red curve), and the composite of AO and PSS (blue curve). (B) FT-IR spectra of pure CTAB (black curve), the composite of PSS and CTAB (red curve), and the composite of AO/PSS after exchanging with CTAB (blue curve).

2. Optimization of experimental parameters

2.1. Optimization of the PSS concentration

In order to obtain the optimal experimental conditions, the peak currents of AO/PSS/PEI modified electrodes prepared with different PSS concentrations were measured before and after incubation with 10 $\mu\text{g mL}^{-1}$ CTAB solution. The difference value of the anodic peak current was calculated using Δi_p ($\Delta i_p = i_0 - i$), where i_0 was the initial peak current response recorded at the AO/PSS/PEI modified electrode and i was the peak current response at the AO/PSS/PEI modified electrodes after the electrodes were treated in different concentrations of CTAB. As shown in Fig. S2A, when the AO concentration was fixed at 200 μM , the difference value of the anodic peak current after incubation with CTAB increased first and then decreased with increasing PSS concentration. The result showed that if the PSS film was too thick, it would cause difficult release of AO from PSS, and the electron transfer rate of AO confined on the modified electrode surface lowered. Finally, 100 μM PSS solution was chosen as the optimal condition for the modification of electrode in the following experiments.

2.2. Optimization of the pH of AO solution

The pH values of AO solution in the range of 2.5 – 10.5 in BR buffer solution were investigated to get the highly sensitive detection of CTAB. As shown in Fig. S2B, the difference value of the anodic peak current after incubation with CTAB increased gradually with increasing the pH up to 8.5 and then decreased. Therefore, pH 8.5 was chosen as the optimum pH for the detection of CTAB in this work.

2.3. Optimization of the reaction time of CTAB

Cyclic voltammetric responses at the AO/PSS/PEI modified electrodes in BR buffer solution (pH 3.5) after the electrodes were immersed in a $10 \mu\text{g mL}^{-1}$ CTAB for different times demonstrate that the cation exchange between surface confined AO and CTAB can reach a balance in 30 min. As shown in Fig. S2C, the difference value of the anodic peak current after incubation with CTAB increased first and then tended to a constant value at the reaction time of 30 min. Therefore, 30 min was used as the reaction time for the CTAB assay in this study.

2.4. Optimization of the pH of buffer solution

The pH value of buffer solution is an important factor that influences the electrochemical reaction. Cyclic voltammetry is used to characterize the effect of solution pH on the electrochemical behavior of CTAB at the AO/PSS/PEI modified electrode. As shown in Fig. S2D, the redox peak currents increased with increasing pH value from 2.5 to 3.5 and then gradually decreased after pH 3.5, Therefore, BR buffer solution with pH 3.5 was used as the supporting electrolyte in all determinations.

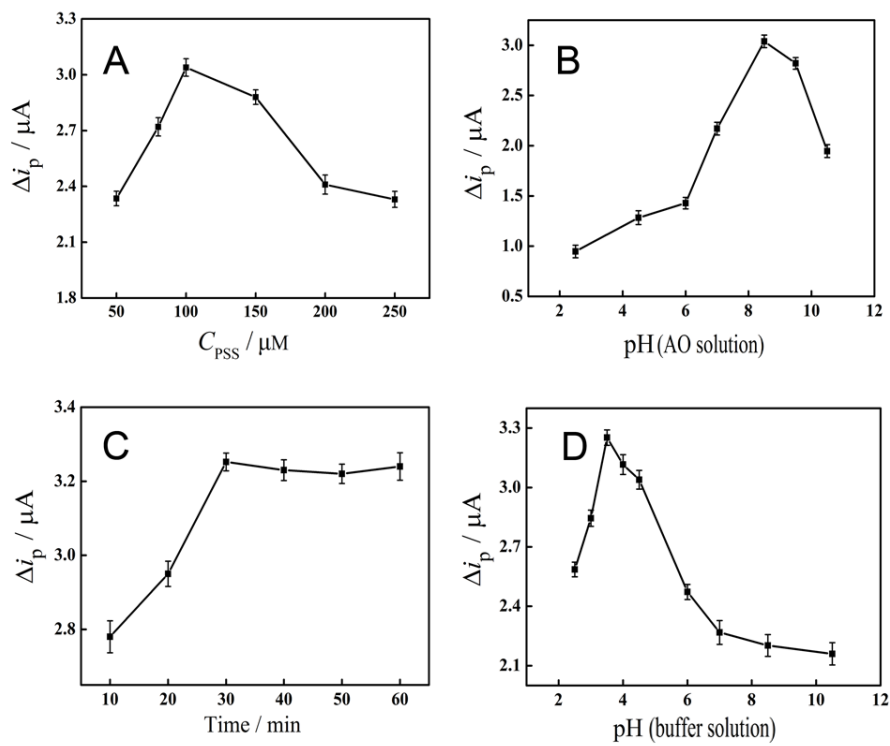


Fig. S2. Effect of the concentration of PSS (A), the pH of AO solution (B), the reaction time of CTAB (C), and the pH of buffer solution (D) on the current response of CTAB.

3. Stability of the sensor

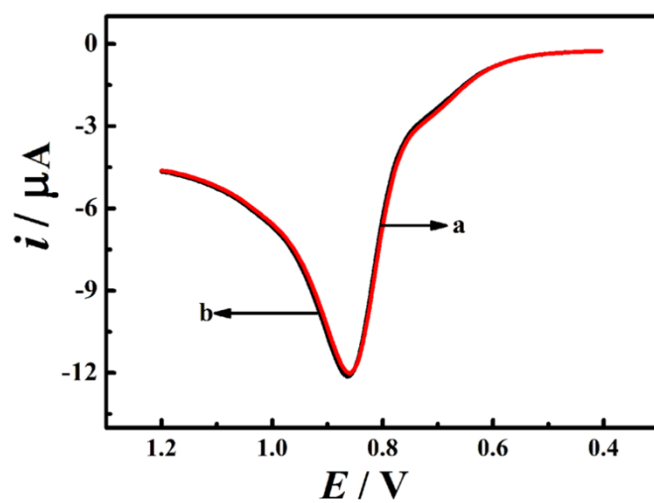


Fig. S3. DPVs in BR buffer solution (pH 3.5) recorded at the AO/PSS/PEI modified electrodes (curve a) and after immersed in 0.10 M PBS (pH 7.0) for 30 min (curve b).

4. Comparison to other detection methods

Table S1 Comparison of the linear range and limit of detection (LOD) of CTAB by different methods.

Method	Linear range ($\mu\text{g mL}^{-1}$)	LOD ($\mu\text{g mL}^{-1}$)	Reference
Fluorimetry	1.82 – 21.9	Not given	1
Titration	0.11 – 1.09	Not given	2
Fluorimetry	0.073 – 2.55	0.018	3
Fluorimetry	7.3 – 10.9	1.09	4
Colorimetry	0.18 – 1.82	Not given	5
Colorimetry	0.2 – 2	0.36	6
Electrochemistry	0.5 – 20	0.3	This work

References

1. J. S. Lundgren, F. V. Bright, *Anal. Chem.*, 1996, **68**, 3377-3381.
2. E. Borrego, D. Sicilia, S. Rubio, D. PeArez-Bendito, *Anal. Chim. Acta*, 1999, **384**, 105-115.
3. X. L. Diao, Y. S. Xia, T. L. Zhang, Y. Li, C. Q. Zhu, *Anal. Bioanal. Chem.*, 2007, **388**, 1191-1197.
4. J. Qian, Y. Xu, S. Zhang, X. Qian, *J. Fluoresc.*, 2011, **21**, 1015-1020.
5. L. Q. Zheng, X. D. Yu, J. J. Xu, H. Y. Chen, *Anal. Methods*, 2014, **6**, 2031-2033.
6. L. Q. Zheng, X. D. Yu, J. J. Xu, H. Y. Chen, *Talanta*, 2014, **118**, 90-95.